International Communications in Heat and Mass Transfer 52 (2014) 121–131

Contents lists available at ScienceDirect

International Communications in Heat and Mass Transfer

journal homepage: www.elsevier.com/locate/ichmt

Influence of geometrical parameters of hexagonal, circular, and rhombus microchannel heat sinks on the thermohydraulic characteristics ☆

A.A. Alfaryjat [a], H.A. Mohammed [b,*], Nor Mariah Adam [a,*], M.K.A. Ariffin [a], M.I. Najafabadi [a]

[a] Department of Mechanical and Manufacturing Engineering, Faculty of Engineering, Universiti Putra Malaysia, 43400 UPM Serdang, Selangor, Malaysia
[b] Department of Thermofluids, Faculty of Mechanical Engineering, Universiti Teknologi Malaysia, 81310 UTM Skudai, Johor Bahru, Malaysia

ARTICLE INFO

Available online 11 January 2014

Keywords:
Microchannel heat sink
Hexagonal microchannel
Circular microchannel
Rhombus microchannel

ABSTRACT

Microchannel heat sink (MCHS) can be done with several cross-section channel shapes. Water flow and heat transfer characteristics are affected by the geometrical parameters of the microchannel which are numerically investigated in this paper. This study covers Reynolds number values in the range of 100–1000 and heat flux is maintained at 500 kW/m^2. Finite volume method (FVM) is used to solve the governing equations and 3D steady state conjugate heat transfer problem. The effects of three different channel shapes (hexagonal, circular, and rhombus) on the MCHS performance are investigated in details. The assessment of MCHS performance is based on a number of exclusive attributes which are temperature profile, heat transfer coefficient, pressure drop, friction factor, and thermal resistance. The results show that the smallest hydraulic diameter of the hexagonal cross-section MCHS has the highest pressure drop and heat transfer coefficient among other shapes. The highest value of the top wall temperature, friction factor and thermal resistance are found with the use of rhombus cross-section MCHS.

1. Introduction

Downscaling of micro-electro-mechanical system (MEMS) advances and devices in microchannel procedure have assisted to drive a way the electronic tools heat flux. The (MEMS) power and growth are necessary to steer the cooling tools in avionics electronics, robotics, and medicine industry. In recent years, the fundamental study of heat transfer and liquid flow in MCHS has been given a significant attention by many researchers. MCHS cooling device was first studied by Tuckerman and Pease [1] in 1981, it was found that if the dimensions of the cooling channel decrease to microscale channel, it led to improve the heat transfer level. Additionally, the heat sinking capability of the silicon microchannels was improved up to forty-fold due to extensive lab experiments which attached the top plat of Pyrex.

Kroeker et al. [2] analyzed numerically the pressure drop in the circular microchannel heat sink and its thermal performance by using the continuum model. Water was used as a working fluid and the Reynolds number was fixed at 500. Their results show that as the heat sink thickness increases, the surface temperature becomes uniform. It was also found that the overall thermal resistance of the heat sink decreases considerably with the decrease of the geometry dimensions, or increase in *Re* number. In another study, Khan et al. [3] carried out experiments in an effort of MCHS performance on the validity of classical correlation of friction factor and temperature profile taking into its account the size of the channel used to predict the behavior of water flow in circular MCHS. It was found that the diameter and the length of the channel have a great influence on the temperature profile of the circular microchannel.

Wu and Cheng [4] experimentally investigated the friction factor value with diverse aspect ratios in silicon straight trapezoidal microchannels. The results yielded that using the same hydraulic microchannel diameter with various cross-sectional shapes can give different results for the friction factor. Wu and Little [5] experimentally investigated the laminar gas friction factors in the trapezoidal cross-section glass microchannels. It was observed that in the laminar flow case, the surface roughness affected the values of the friction factors which are different from the conventional microchannel flow.

An experimental study was carried out on the pressure drop laminar flow and water heat transfer in 13 diverse trapezoidal silicon microchannels by Wu and Cheng [6]. It was concluded that using different geometric factors would influence the values of Nusselt number and friction factor. The apparent friction and laminar Nusselt number increase with the increase of surface hydrophilic property and surface roughness. In another study, Weilin et al. [7,8] experimentally studied the water flow characteristics across trapezoidal silicon microchannels. Their results show that the conventional laminar current, because of the effect of the microchannel surface roughness, is much lower than the pressure drop and flow friction in microchannel shapes.

Arkilic et al. [9] studied experimentally the helium rarefaction and gaseous flow in long cross-section channels. The results show that for the no-slip flow regime, the pressure drop through the microchannel was higher than the system with slip flow. Another experimental study was

☆ Communicated by W.J. Minkowycz.

* Corresponding authors.
E-mail addresses: Hussein.dash@yahoo.com (H.A. Mohammed), mariah@eng.upm.edu.my (N.M. Adam).

0735-1933/$ – see front matter © 2014 Elsevier Ltd. All rights reserved.
http://dx.doi.org/10.1016/j.icheatmasstransfer.2014.01.015

Nomenclature

A	channel flow area, (m^2)
A_c	area of the cross-section of the channel, (m^2)
B	half height of the hexagon, (m)
C	half width of the hexagon, (m)
C_p	specific heat, (J/kg·K)
D	edge length of the hexagon, (m)
D	diameter of the circular, (m)
D_h	hydraulic diameter, (m)
f	friction factor
H_{hs}	depth of heat sink, (m)
k	thermal conductivity, (W/m·K)
κ_s	solid thermal conductivity, (W/m·K)
L_{ch}	length of channel, (m)
L_{hs}	length of heat sink, (m)
N	number of channels
P	channel wet perimeter, (m)
P	channel high of the rhombus, (m)
$\hat{p}$	dimensionless pressure
Pr	Prandtl number
Q	channel width of the rhombus, (m)
q_w	heat flux at the top plat of microchannel heat sink, (kW/m^2)
Re	Reynolds number
R_{th}	thermal resistance
S	distance between two microchannels, (m)
T_{max}	maximum temperature, (K)
T_f	fluid temperature, (K)
T_{in}	inlet temperature fluid, (K)
T_w	wall temperature, (K)
u_{in}	inlet fluid velocity, (m/s)
U	dimensionless velocity in X-coordinate
$V°$	total volume flow rate
V	dimensionless velocity in Y-coordinate
W	dimensionless velocity in Z-coordinate
W_{hs}	width of heat sink, (m)
X	channel hypotenuse of the rhombus, (m)
X,Y,Z	dimensionless Cartesian coordinates
ΔP	Pressure drop

Greek symbols

Φ	channel angle
μ	viscosity, (kg·m/s)
ρ	density, (kg/m^3)
θ	dimensionless temperature, $\theta = \theta = T_f - T_i/T_w - T_i$

Subscripts

ch	channel
f	fluid
h	hydraulic
in	inlet
hs	heat sink
s	solid
w	wall

conducted by Peng and Peterson [10] to investigate the convective heat transfer and pressure drop for water current in rectangular shape MCHS. It was concluded that the flow characteristic and convective heat transfer had an important influence by the geometrical parameters. It was also found that the laminar flow and the heat transfer were reliant on the aspect ratio and hydraulic channel diameter ratio of the microchannel. Moreover, the fluid flow affects the rectangular cross-section MCHS cooling performance was also outlined by Choi and Cho [11].

Heat transfer value and laminar liquid-water flow through wavy MCHS with rectangular shape were numerically studied by Sui et al. [12]. The simulation results stated that the Dean vortex patterns may change considerably along the flow channel direction. The high heat transfer values can be found in the long channel fluid direction of the wavy microchannel. Extending this study, Mohammed et al. [13] investigated numerically the water flow characteristics and heat transfer in wavy MCHS (WMCHS). The results show that wavy microchannel has better heat transfer performance than the straight microchannels. It was also found that as the wavy amplitude decreases, the temperature of the MCHS increases and it is lower than the straight MCHS. Judy et al. [14] investigated experimentally the pressure driven liquid flow through square and round microchannels. It was indicated that an increase in viscosity led to increasing the pressure drop and decreasing the friction factor product at higher *Re* number. The fluid and heat transfer for four heated microchannels was studied numerically by Toh et al. [15]. It was concluded that at lower Reynolds number, water viscosity value and frictional losses lead to raise the water temperature in the microchannel.

Aghanajafi et al. [16] and Shams et al. [17] carried out a numerical simulation of fully developed laminar slip gas flow characteristics and heat transfer in rhombus microchannels. It was concluded that the maximum gas velocity decreases when the aspect ratio of the channel increases. The results also show that the value of the Nusselt number became more significant when the Reynolds number decreases unlike the moderate Reynolds number which has no effect on the Nusselt number. Gunnasegaran et al. [18] conducted a numerical investigation that analyzes the impact of geometrical parameters of trapezoidal, rectangular and triangular MCHS for Reynolds number in the range of 100–1000. It was found that the rectangular shaped MCHS gives the best heat transfer enhancement value followed by trapezoidal and triangular MCHS. In a separate study, Tamayol and Bahrami [19] analyzed numerically the laminar water fully developed within micro–minichannels of regular polygonal and hyper elliptical cross sections. The numerical results show that hexagonal ducts have the minimum pressure drop in comparison with other polygonal shapes.

Chein and Chen [20] studied numerically the heat transfer enhancement and fluid flow for different inlet and outlet water arrangements in MCHS with rectangular cross section. They indicated that low-temperature happens in the region where microchannel heat sink is placed, notably at the entrance of the channels. The inlet and the outlet locations affected the temperature distribution in the heat sink. In a different study, Chiu et al. [21] studied experimentally and numerically the effects of the pressure drop and channel geometry on the heat transfer performance of microchannel heat sink. It was indicated that the pressure drop increased when the flow rate increased. Moreover, the high temperature zone was not affected by changing the pressure drop or the geometry dimensions of the channel. Li et al. [22] studied numerically forced convection heat transfer in a silicon MCHS. It was concluded that the thermophysical properties of the fluid flow can considerably influence both the heat transfer and fluid flow in MCHS. The effect of MCHS geometry shapes was studied numerically by Li and Peterson [23]. It was found that both substrate thermo-physical properties and the microchannel physical geometry are very significant parameters in MCHS design and optimization. Qu and Mudawar [24] numerically investigated the fluid water flow and heat transfer enhancement through rectangular MCHS. The highest point temperature was noticed at the heated surface of the heat sink. In addition, the Nusselt number and heat flux have high values next to the inlet channel. It was also found that the length of the flow developing area is affected by Reynolds number. The polymeric MCHS thermal performance which is invented for small plane cooling surfaces was numerically investigated by Barba et al. [25]. Their results show that the thermal resistance decreases considerably when the mass flow rate increases. Other recent works on MCHS with different shapes can be found in Refs. [26–33].

From the above literature review, it is clear to see that MCHS was studied widely but the research of MCHS performance with different cross-section channel shapes such as circular, hexagonal, and rhombus is very limited and there is no extensive study to examine the channel shape effect on the heat transfer and fluid flow characteristics of MCHS. Moreover, the past research has not given a great attention to the MCHS case using various channel shapes, and this has motivated the present study. The current study is aimed to investigate numerically the effect of different channel shapes and the geometrical parameters on the hydraulic and thermal water flow performance of MCHS. Reynolds number, for all flow channel shapes is employed in the range of 100–1000. The assessment of MCHS performance is based on a number of exclusive attributes which are dimensionless temperature profile, heat transfer coefficient, pressure drop, friction factor, and thermal resistance and it is presented and interpreted in this paper.

2. Numerical model

2.1. MCHS model

The schematic diagrams of the geometrical shape of the microchannel heat sinks are shown in Fig. 1. The size of microchannel heat sink is fixed at $W_{hs} = 22$ mm, $L_{hs} = 12$ mm, and $H_{hs} = 1.5$ mm. The width of the edges of the heat sink is maintained at 1 mm. In this paper, hexagonal, circular, and rhombus cross-section microchannels were examined. The height of the channels is varied from 200–300 μm. The water flows through a number of microchannels and the heat flux is supplied at the heat sink top plate. The dimensions of three different channels of each cross-section shape of microchannels are given in Tables 1–3. The results of the heat transfer enhancement which is affected by the geometrical shape parameters of the microchannel heat sink with distinct channel shapes were presented.

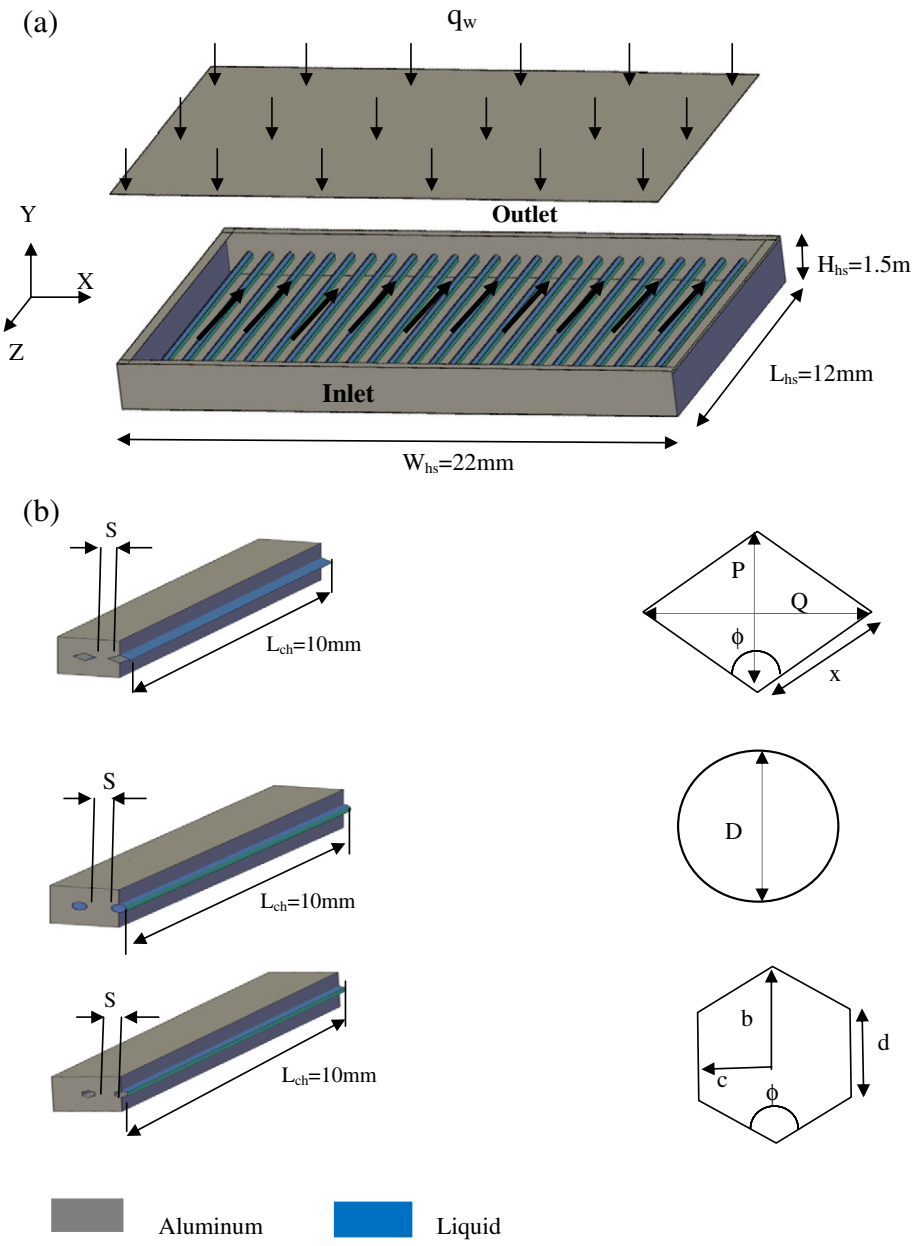

Fig. 1. (a) Schematic diagram of the computational domain, (b) sections of the rhombus, circular, and hexagonal cross-section MCHS with its dimensions.

Table 1
Dimensions of three different sets of hexagonal cross-section MCHS.

	Case 1	Case 2	Case 3
c (μm)	90	110	130
b (μm)	100	120	150
d (μm)	100	125	150
ϕ (μm)	120	120	120
L_{ch} (μm)	10,000	10,000	10,000
S (μm)	613	571	530
D_h (μm)	170	216	260
Number of channel	26	26	26

2.2. Governing equations

The heat of the microchannel is transferred from the fluid flow to the wall. In order to examine the water utilization on different geometrical parameters of MCHS cooling performance, the following assumptions are adopted: (i) Both heat transfer and fluid flow in MCHS are in three dimensional and steady-state; (ii) fluid flow is incompressible, single phase, and laminar flow; (iii) the physical properties of both fluid flow and heat sink materials are temperature independent; and (iv) all the surrounding surfaces of MCHS are adiabatic except for the microchannel top plate which is exposed to heat flux. Based on the above assumptions, the continuity, momentum and energy equations for this study can be written as [34]:

Continuity equation:

$$\frac{\partial U}{\partial X}+\frac{\partial V}{\partial Y}+\frac{\partial W}{\partial Z}=0. \tag{1}$$

X-momentum equation:

$$U\frac{\partial U}{\partial X}+V\frac{\partial U}{\partial Y}+W\frac{\partial U}{\partial Z}=-\frac{d\hat{p}}{dX}+\frac{1}{\mathrm{Re}}\left(\frac{\partial^2 U}{\partial X^2}+\frac{\partial^2 U}{\partial Y^2}+\frac{\partial^2 U}{\partial Z^2}\right). \tag{2}$$

Y-momentum equation:

$$U\frac{\partial V}{\partial X}+V\frac{\partial V}{\partial Y}+W\frac{\partial V}{\partial Z}=-\frac{d\hat{p}}{dY}+\frac{1}{\mathrm{Re}}\left(\frac{\partial^2 V}{\partial X^2}+\frac{\partial^2 V}{\partial Y^2}+\frac{\partial^2 V}{\partial Z^2}\right). \tag{3}$$

Z-momentum equation:

$$U\frac{\partial W}{\partial X}+V\frac{\partial W}{\partial Y}+W\frac{\partial W}{\partial Z}=-\frac{d\hat{p}}{dz}+\frac{1}{\mathrm{Re}}\left(\frac{\partial^2 W}{\partial X^2}+\frac{\partial^2 W}{\partial Y^2}+\frac{\partial^2 W}{\partial Z^2}\right). \tag{4}$$

Energy equation

$$U\frac{\partial \theta}{\partial X}+V\frac{\partial \theta}{\partial Y}+W\frac{\partial \theta}{\partial Z}=\frac{1}{\mathrm{Re.Pr}}\left(\frac{\partial^2 \theta}{\partial X^2}+\frac{\partial^2 \theta}{\partial Y^2}+\frac{\partial^2 \theta}{\partial Z^2}\right). \tag{5}$$

The dimensionless parameters are:

$$\mathrm{X}=\frac{x}{D_h},\ \mathrm{Y}=\frac{y}{D_h},\ \mathrm{Z}=\frac{z}{D_h},\ \mathrm{U}=\frac{u}{u_{in}},\ \mathrm{V}=\frac{v}{u_{in}},\ \mathrm{W}=\frac{w}{u_{in}},\ \theta=T_f-T_{in}/T_w-T_{in}.$$

Table 2
Dimensions of three different sets of circular cross-section MCHS.

	Case 1	Case 2	Case 3
D (μm)	200	250	300
L_{ch} (μm)	10,000	10,000	10,000
S (μm)	590	540	488
D_h (μm)	200	250	300
Number of channel	26	26	26

Table 3
Dimensions of three different sets of rhombus cross-section MCHS.

	Case 1	Case 2	Case 3
Q (μm)	200	250	300
p (μm)	340	440	540
x (μm)	200	250	300
ϕ (μm)	60	60	60
L_{ch} (μm)	10,000	10,000	10,000
S (μm)	447	343	259
D_h (μm)	170	216	260
Number of channel	26	26	26

The channel heat sink entrance is assumed at Z = 0, as it can be seen in Fig. 1. There are two important kinds of boundary conditions in these studies which are water flows through the microchannel heat sink and the top surface removes the heat. The rest part of the channel entry is made of aluminum. The temperature of the inlet water is 290 K and the inlet water velocity in microchannel depends on the Reynolds number value. In this paper, the range of the Reynolds number is from 100 to 1000. The top plate heat flux of the heat sink is maintained at 500 kW/m^2. The solid and water physical properties used in the computation are ρ = 998.2 kg/m^3, C_p = 4182 J/kg·K, μ = 0.001003 kg/m s, κ = 0.6 W/m·K, and κs = 202.4 W/m·K.

2.3. Grid testing and model validation

A grid independence test was conducted to assess the effect of the grid size numbers. Three sets of mesh were produced using hexagonal elements with 250,000 nodes, 610,000 nodes, and 810,000 nodes. Fig. 2 shows the result of the heat transfer coefficient with Reynolds number ranged from 100 to 1000. It can be noticed that the values of heat transfer coefficient of 610,000 and 810,000 are almost equal. Therefore, the computation with 610,000 grids is used for all the numerical computations presented in this paper.

The code validation was done based on the boundary conditions and microchannel geometry which were first used by Gunnasegaran et al. [18]. They used water as a working fluid at Reynolds number = 500 and the heat flux = 500 kW/m^2. As it can be seen in Fig. 3a the temperature profile results are in good agreement with Gunnasegaran et al. [18]. The code was further validated by comparing the present results with the results of Gunnasegaran et al. [35] as shown in Fig. 3b. It can be seen that the pressure drop values fall between the accepted ranges.

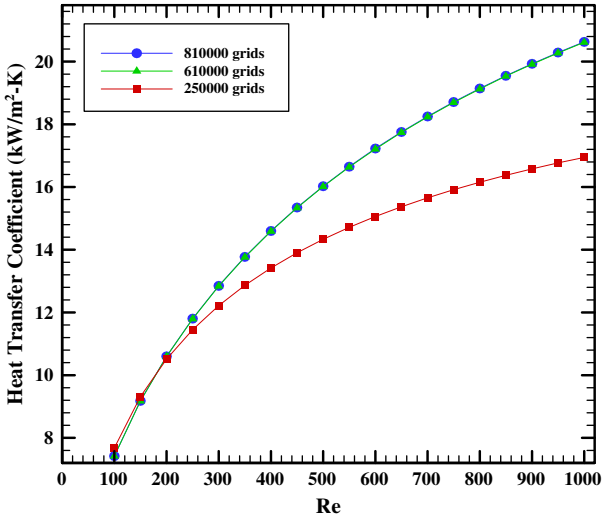

Fig. 2. Heat transfer coefficient for different Reynolds numbers for hexagonal cross-section MCHS (D_h = 0.26 mm) using three different grids.

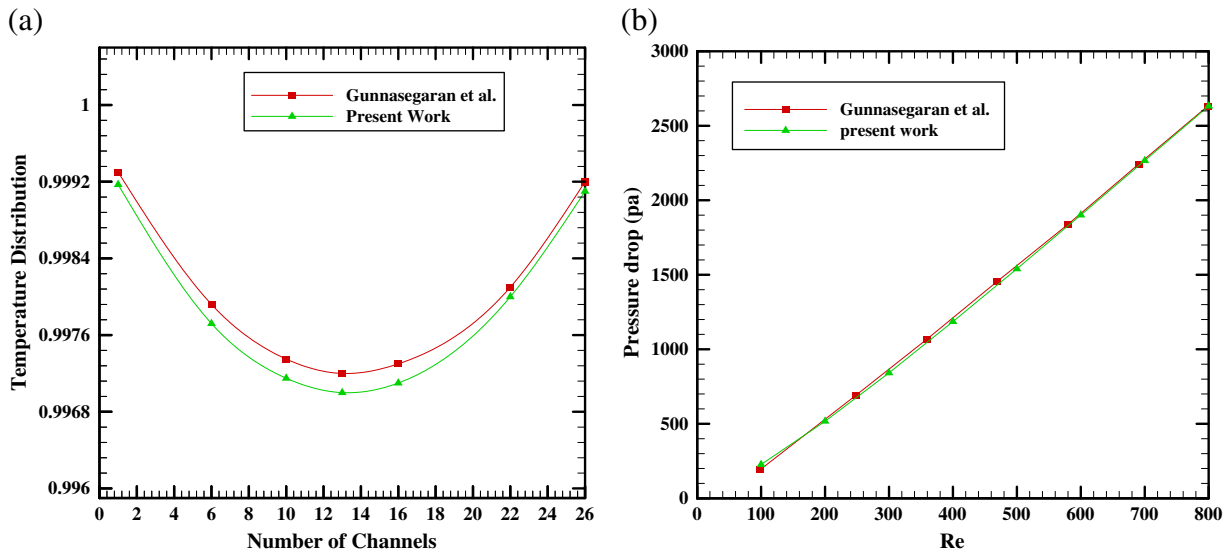

Fig. 3. Comparison of the present results with the results of Gunnasegaran et al. [18,35] for rectangular cross-section MCHS, (a) the variation of temperature distribution with number of channels, (b) the variation of pressure drop with different Reynolds numbers.

2.4. Numerical procedures

Finite volume method (FVM) is used to perform the numerical calculations by solving the governing equations along with the boundary conditions. The single phase domain conjugate heat transfer problem was used to solve the fluid and solid phase equations. SIMPLE algorithm was used to solve the flow field [36]. The second-order upwind differencing scheme is implemented to solve the convective terms. This is an iterative solution procedure initialized by predicting the fluid field pressure. The pressure drop is efficient to use the continuity equation. Even the pressure drop is not found in the continuity equation, it is easy to be changed through the pressure equation corrections. The iterations were continued until the sum of residuals turn into negligible (less than 10^{-7}) and the iteration of velocity components became constant. Finally, solving the equation of the energy leads to calculate the temperature value.

3. Results and discussion

The influence of channel shapes such as hexagonal, circular, and rhombus on the MCHS thermal and hydrodynamic performance by using water as a working fluid is analyzed. The Reynolds number is employed in the range of 100 to 1000 for all channel flow shapes. The heat flux on top wall of MCHS is maintained at 500 kW/m^2.

3.1. Dimensionless temperature

The dimensionless temperature for hexagonal cross-section microchannel at $Re = 500$ and $q_w = 500$ kW/m^2 is presented in Fig. 4a. It can be seen that the extreme dimensionless temperature region took place at the edge of the MCHS since the heat inside the channels is dissipated by convection fluid flow while the low point temperature area occurred where the microchannel is located, particularly at the middle part of the MCHS due to the high heat transfer coefficient. The temperature profiles decrease when L/D_h increases and the trend is the same for each cross sectional shape of MCHS. The dimensionless temperature profile for each microchannel can be calculated using the following equation [37]:

$$\theta = \frac{T_f - T_{in}}{T_w - T_{in}} \tag{6}$$

where T_f is the fluid temperature, T_w is the wall temperature, and T_{in} is the inlet temperature.

The water temperature inside the channels and near to the side of the MCHS is higher this is due to the high heat transfer at the sides of the MCHS. Fig. 4b shows the temperature contours of the top wall temperature of the hexagonal cross-section MCHS with $c = 90$ μm, $b = 100$ μm, $\phi = 120$ and $Re = 500$. For all types of microchannel heat sink studied, it is observed that the maximum temperature occurs at the side walls while the lowest temperature occurs in the middle of the MCHS.

The temperature profile distribution for various Reynolds numbers for hexagonal, circular, and rhombus shapes using the smaller hydraulic diameter is presented in Fig. 4c. It can be seen that rhombus cross-section shape has the lowest temperature; this mainly attributed to area of the rhombus cross sectional MCHS which has better heat transfer between the fluid and solid. The MCHS of circular cross-section has the highest value. While, the value of the temperature profile of the hexagonal cross-section MCHS is in between the circular and rhombus. Moreover, the results show that as Reynolds number increases, the temperature decreases linearly. Fig. 4d shows the top wall temperature for various Reynolds numbers for hexagonal, circular, and rhombus shapes using the smaller hydraulic diameter. It can be seen that rhombus cross-section shape has the lowest temperature. The MCHS of circular cross-section has the highest value. While, the value of the temperature of the hexagonal cross-section MCHS is in between the circular and rhombus. The temperature of the top wall of the MCHS decreases as the Reynolds number increases.

The decrease of velocity causes the kinetic energy along the channel to decrease in order to satisfy the needs of energy conservation equation. Consequently, the temperature along the channel flow direction should raise [18]. Fig. 5a shows the temperature of water along the length of channel number 1 and channel number 14 of the hexagonal shape. The results show that the temperature of both channels increases along the flow direction. By using hydraulic diameter $D_h = 170$, $Re = 500$, and $Q = 500$ kW/m^2, it is noted that the temperature of channel number 14, the middle channel of MCHS is lower than channel number 1.

The water temperature increases between the channel outlet and inlet of the MCHS for the hexagonal cross-section with different hydraulic diameters of 170, 216, and 260 μm, channel length = 1000 μm and $q_w = 500$ kW/m^2 as shown in Fig. 5b. As expected, for constant water inlet temperature and heat flux, the outlet temperature value of the water decreases with the increase of Reynolds number. Fig. 5b shows the fluid temperature rise with the increase of Reynolds number; this

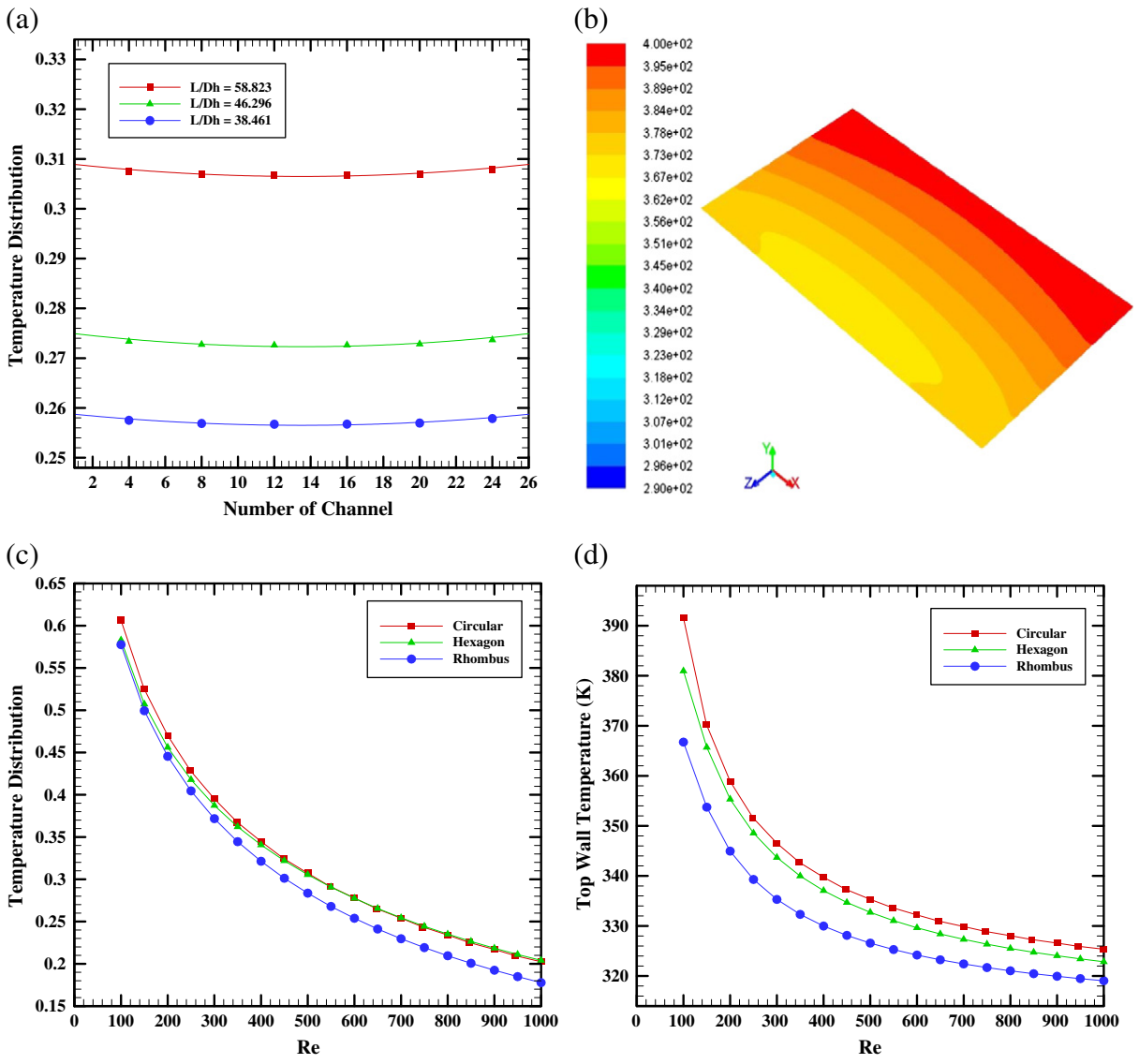

Fig. 4. (a) Average temperature profile for each channel for hexagonal cross-section MCHS, (b) temperature contour of the hexagonal cross-section MCHS, (c) average temperature profile for various Reynolds numbers for different cross-section shapes of MCHS, (d) top wall temperature for various Reynolds numbers for different cross-section shapes of MCHS.

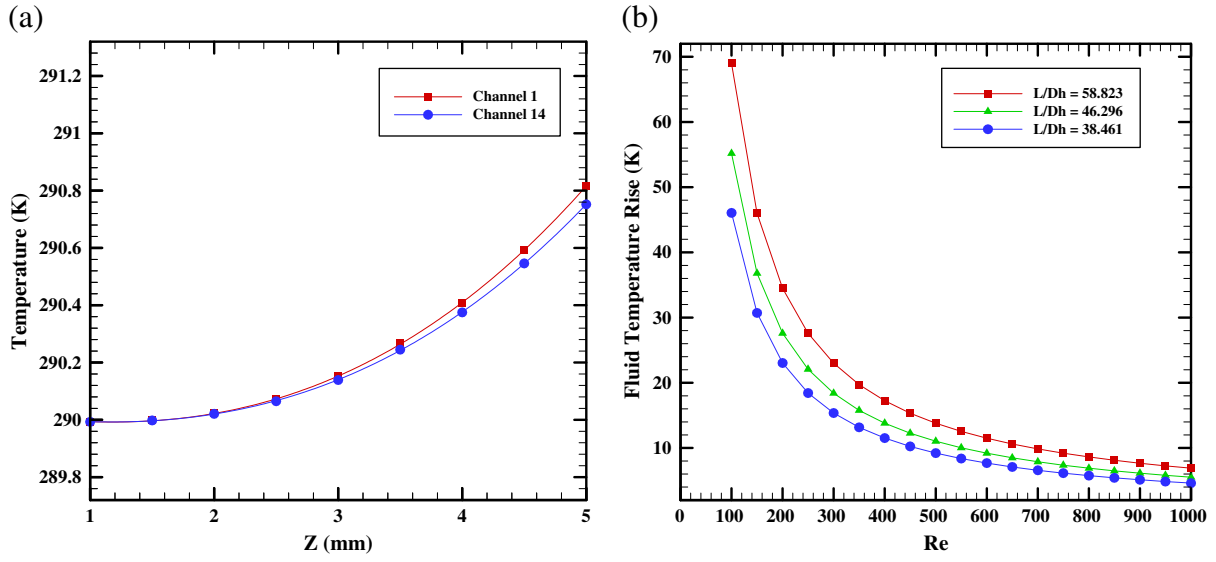

Fig. 5. (a) Water temperature along the length of the channel, (b) fluid temperature rise versus Reynolds number for hexagonal cross-section MCHS.

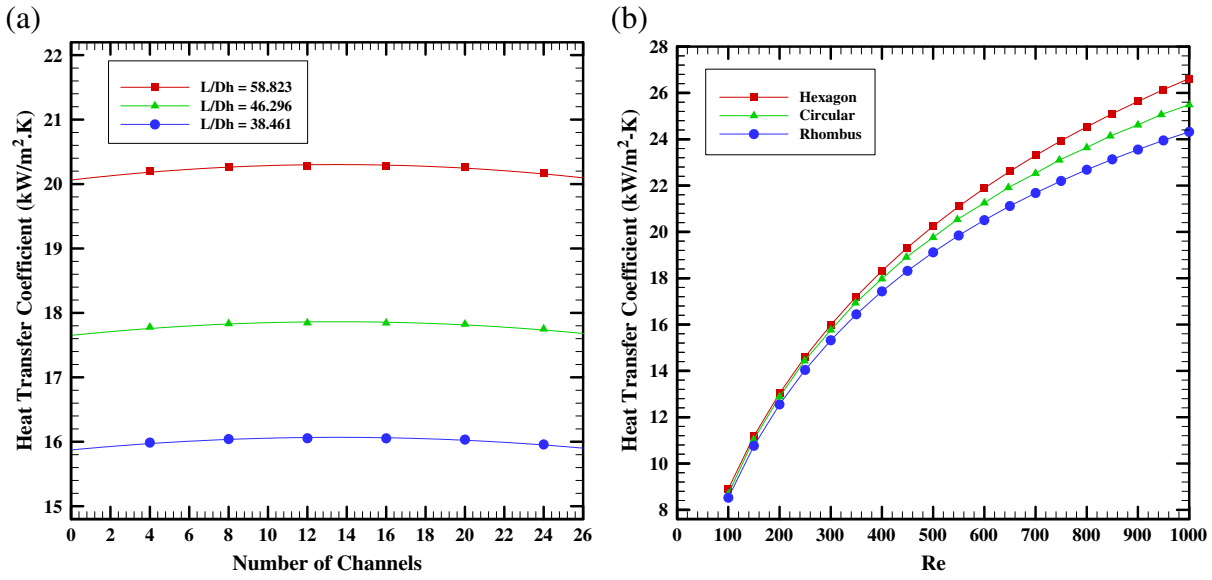

Fig. 6. (a) Average heat transfer coefficient in each channel of the hexagonal cross-section MCHS, (b) average heat transfer coefficient for different cross-sectional shapes of the MCHS.

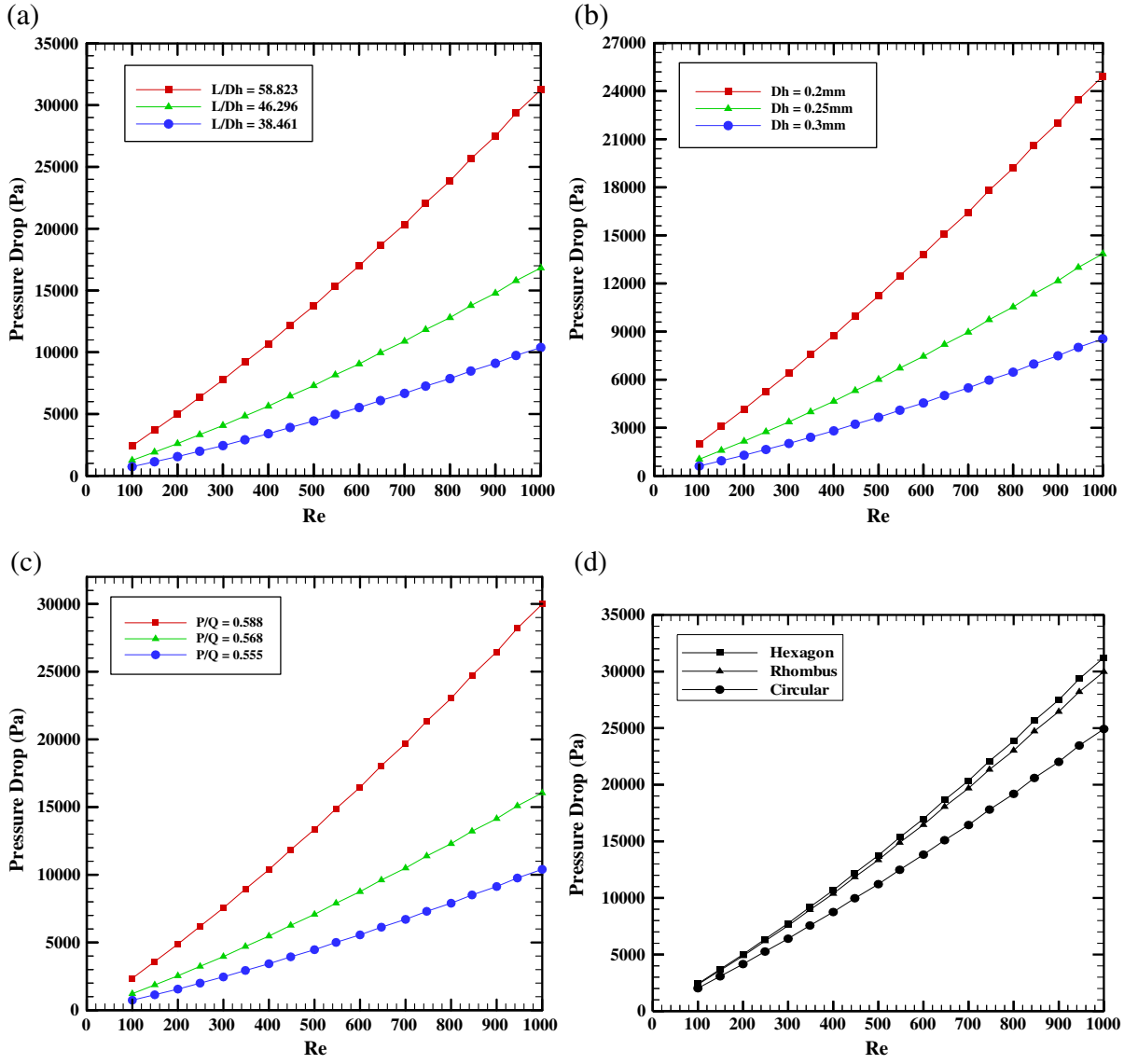

Fig. 7. Pressure drop variation versus Reynolds number for, (a) hexagonal cross-section MCHS, (b) circular cross-section MCHS, (c) rhombus cross-section MCHS, (d) different cross-sectional shapes of the MCHS.

is due to the huge quantity of fluid which carried the same amount of heat. The trend of the present results agreed qualitatively with the results obtained by Ambatipudi and Rahman [38].

3.2. Heat transfer coefficient

The averaged heat transfer coefficient of the hexagonal cross-section MCHS for various hydraulic diameters is illustrated in Fig. 6a. While the L/D_h decreases, the heat transfer coefficient value decreases; the trends of the results are the same for each cross sectional shape of the MCHS. The highest heat transfer coefficient is found with the smaller channel; this is due to the lower pressure drop in larger channel diameter which has lower inlet velocity driven into MCHS [18]. The middle channel (channel number 14) has the highest value of the averaged heat transfer coefficient as expected. For other channels, the average heat transfer coefficient value decreased continuously based on their distances from the channel wall. It can be seen that the lowest heat transfer coefficient is close to the edge.

The calculated average heat transfer coefficient with various Reynolds numbers for different cross sectional shapes MCHS is presented in Fig. 6b. This figure shows that the heat transfer coefficient value for hexagonal cross-section MCHS has the highest value at $q_w = 500$ kW/m^2 and $Re = 500$. Rhombus cross-section MCHS has the lowest value of heat transfer coefficient, while circular cross-section MCHS lies in between the hexagonal and rhombus MCHS. The area of the hexagonal cross-section MCHS has an advantage of improving the heat transfer coefficient than the circular and rhombus channels. It can be noted that the heat transfer coefficient increases for each cross-section shape MCHS with the increase of Reynolds number.

3.3. Pressure drop

The pressure drop effects on the MCHS performance for the hexagonal, circular, and rhombus cross-sections respectively are depicted in Fig. 7a–c. The region of high pressure is located at the channel entrance and the channel outlet has the lowest pressure drop. This is due to the constant inlet velocity and heat flux for a fixed hydraulic diameter for a fully developed channel flow in the present study. The fluid kinetic energy causes an increase in minor loses, which is found to be equivalent to the Reynolds number square [35]. It is also found that the water

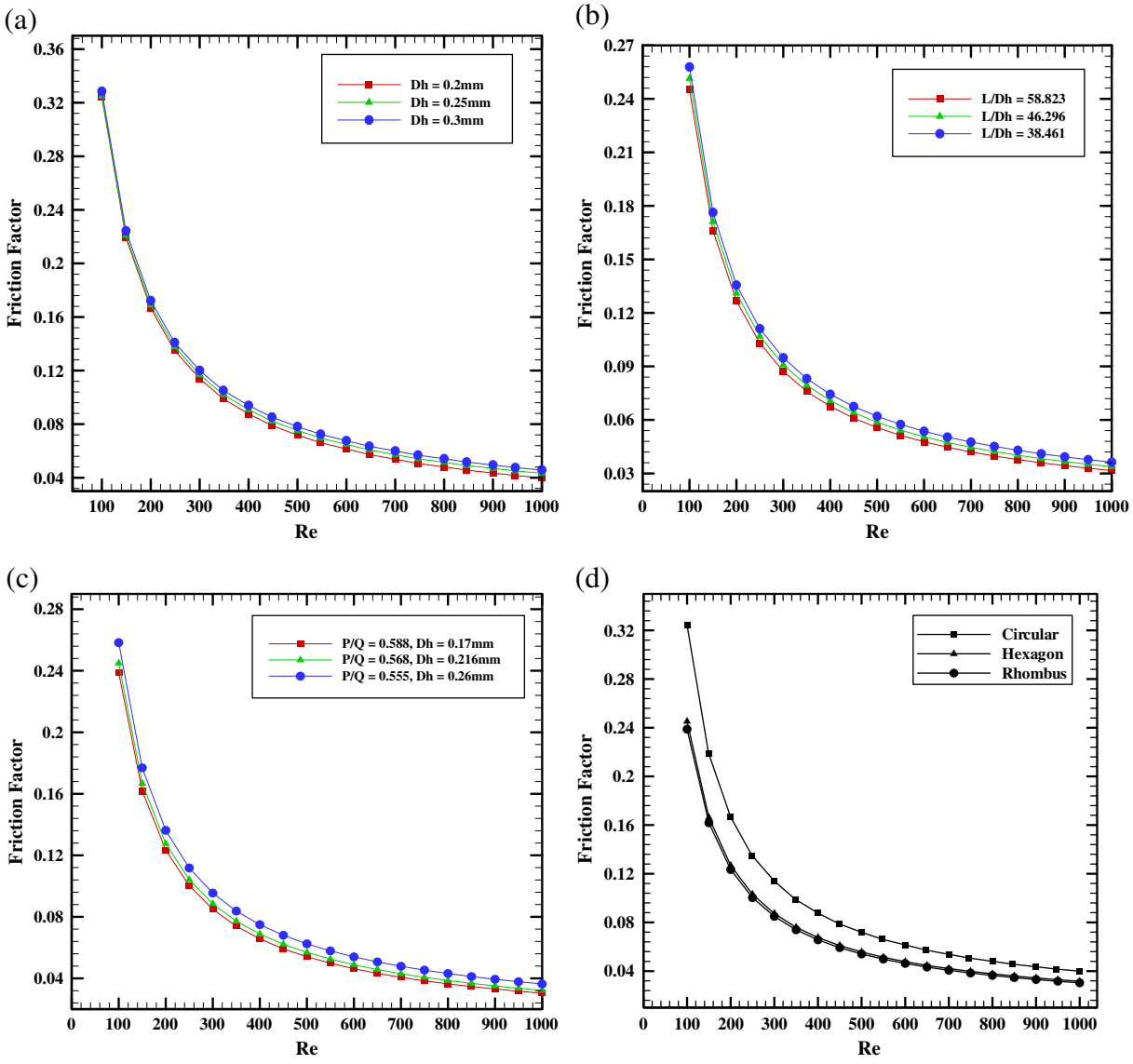

Fig. 8. Friction factor at different length-hydraulic diameter ratios for (a) hexagonal cross-section MCHS, (b) circular cross-section MCHS, (c) rhombus cross-section MCHS, (d) different cross-sectional shapes of the MCHS.

pressure drop variation of microchannels increases when the hydraulic channel's diameter decreases; this is related to the fact that forcing a liquid through a small hydraulic diameter channel produced a higher pressure drop compared to larger hydraulic diameter. From Fig. 7d, it is also noticed that the pressure drop for the smallest channel for hexagonal cross-section microchannel is the highest, for circular cross-section microchannel is the smallest than other shapes, and for rhombus cross-section microchannel is in between the two channel shapes.

3.4. Friction factor

Friction factor variation, f, for hexagonal, circular, and rhombus cross-section shape microchannels versus Reynolds number is shown in Fig. 8a–c. The friction factor for different MCHS cross sections using Darcy equation [39] is given by:

$$f = \frac{2D_h}{pu_{in}^2}\frac{\Delta p}{L_{ch}} \tag{7}$$

where D_h is the hydraulic diameter, Δp is the pressure drop, ρ is the water density, u_{in} is the inlet velocity of the water, and L_{ch} is the length of channel.

The results show that the flow behavior is very similar for all types of cross-sectional shapes of the MCHS where the friction factor in microchannels decreases with the increase of Reynolds number. In overall, it can be noticed from Fig.8d that the circular cross-section MCHS has the most friction factor, for the hexagonal cross-section MCHS is the least, and rhombus cross-section is in between. This may be due to the high pressure drop of the hexagonal cross-section compared with the rhombus cross-section. In MCHS having equal channel hydraulic diameter with different cross-sectional shapes, the friction factor of water flowing in microchannels can be very much different.

3.5. Thermal resistance

MCHS water cooling performance is evaluated by finding the thermal resistance (R_{th}) which depends on temperature inlet fluid (T_{in}) and maximum wall heat sink temperature ($T_{w,\,max}$). Thermal resistance can be calculated using the following equation [40]:

$$R = \frac{T_{\max} - T_{in}}{q_w}. \tag{8}$$

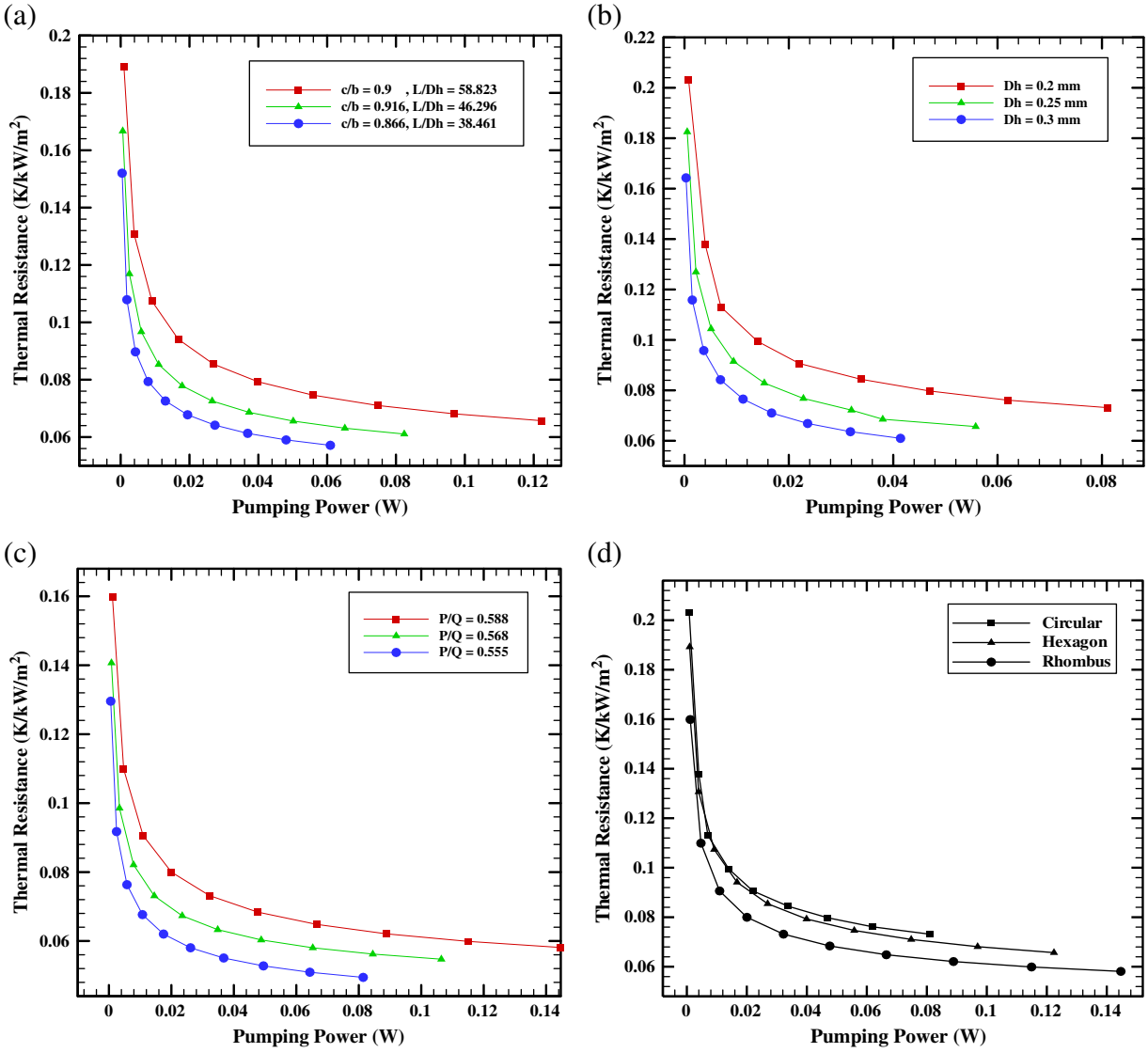

Fig. 9. Thermal resistance at different length-hydraulic diameter ratios for (a) hexagonal cross-section MCHS, (b) circular cross-section MCHS, (c) rhombus cross-section MCHS, (d) different cross-sectional shapes of the MCHS.

Since the maximum wall heat sink temperature of rhombus cross-section MCHS is lower than the hexagonal and circular cross-section MCHS, the lower thermal resistance is then expected in rhombus cross-section MCHS. The pressure drop and area of MCHS which relates to the pumping power are considered as main parameters in MCHS operation. To find out how the dimensional parameters affect the thermal performance, an optimal analysis should be used to compare the thermal resistance for different MCHS shapes. The pumping power, P, is defined as [41]:

$$\overline{p} = \dot{V} \cdot \Delta P = N \cdot u_m \cdot A_c \cdot \Delta p \tag{9}$$

where $\dot{V}$ is the total volume flow rate; A_c is the area cross-section of the channel; u_m is the mean velocity in the channel; N is the number of channels; and ΔP is the pressure drop across the channel.

The areas of the hexagon, circular and rhombus cross-section shapes of MCHS are defined as:

$$A_{\text{hexagon}} = \frac{3}{2} \cdot \sqrt{3} \cdot d^2 \ , \ A_{\text{circular}} = \pi r^2 \ , \ A_{\text{rhombus}} = \frac{1}{2} \cdot P \cdot Q.$$

The cooling performance of the MCHS using water as a working fluid is determined by obtaining the results of the thermal resistance as depicted in Fig. 9a–c. It is clearly seen that the thermal resistance increases with the decrease of the hydraulic diameter of the channel. Furthermore, the larger hydraulic diameter of the channel has the lowest R_{th} and the smaller hydraulic diameter shows the highest value. The results also show that the flow behavior is very similar for all types of cross sectional shapes of MCHS where the R_{th} decreases as Reynolds number increases. It is evident from these figures that the R_{th} of rhombus cross-section MCHS is lowest followed by the hexagonal and circular MCHS. The maximum reduction in R_{th} of the rhombus is about 0.16 K/kW/m^2 and the pumping power is 0.145 W as shown in Fig. 9d. Thus, a MCHS of the rhombus cross-section is capable of removing the heat flux between the top wall temperature and the inlet temperature of MCHS by using smaller channel than the hexagonal and circular cross-section MCHS. Therefore, it can be proposed that rhombus cross-section shape MCHS is the best cooling device geometry for removing high heat flux which can be used to develop the next generation technology.

4. Conclusions

Numerical simulation on the heat transfer and water flow characteristics in MCHS was carried out in this present paper. Three channel shapes are considered (hexagonal, circular, and rhombus) along with its geometrical parameters were examined. According to the above simulated results, the following conclusions can be drawn:

- Rhombus cross-section MCHS has the lowest temperature and lower top wall temperature than other channel shapes studied.
- The smallest channel of the hexagonal cross-section MCHS has the highest heat transfer coefficient among other channel shapes studied followed by circular and rhombus cross-section MCHS.
- The hexagonal cross-section MCHS has the most value of the pressure drop, the circular cross-section has the least, and the rhombus is in between.
- The rhombus cross-section MCHS has the lowest friction factor and the thermal resistance followed by the hexagonal and circular MCHS.
- Thus, hexagonal cross-section MCHS has the privilege to be the best channel shape for the heat transfer coefficient and pressure drop. However, rhombus cross-section MCHS is the best channel in terms of temperature, friction factor, and thermal resistance.

References

[1] D.B. Tuckerman, R.F. Pease, High performance heat sinking for VLSI, IEEE Electron Device Lett. EDL-2 (1981) 126–129.

[2] C.J. Kroeker, H.M. Soliman, S.J. Ormiston, Three-dimensional thermal analysis of heat sinks with circular cooling micro-channels, Int. J. Heat Mass Transf. 47 (2004) 4733–4744.

[3] M.N. Khan, M. Islam, M.M. Hasan, Experimental approach to study friction factor and temperature profiles of fluid flow in circular microchannels, J. Mech. Eng. Res. 3 (2011) 209–217.

[4] H.Y. Wu, P. Cheng, Friction factors in smooth trapezoidal silicon microchannels with different aspect ratios, Int. J. Heat Mass Transf. 46 (2003) 2519–2525.

[5] P.Y. Wu, W.A. Little, Measurement of friction factors for the flow of gases in very fine channels used for microminiature Joule–Thomson refrigerators, Cryogenics 24 (1983) 273–277.

[6] H.Y. Wu, P. Cheng, An experimental study of convective heat transfer in silicon microchannels with different surface conditions, Int. J. Heat Mass Transf. 46 (2003) 2547–2556.

[7] Q. Weilin, G.M. Mala, L. Dongqing, Pressure-driven water flows in trapezoidal silicon microchannels, Int. J. Heat Mass Transf. 43 (1999) 353–364.

[8] Q. Weilin, G.M. Mala, L. Dongqing, Heat transfer for water flow in trapezoidal silicon microchannels, Int. J. Heat Mass Transf. 43 (2000) 3925–3936.

[9] E.B. Arkilic, K.S. Breuer, M.A. Schmidt, Gaseous slip flow in long microchannels, J. Microelectromech. Syst. 6 (1997) 167–178.

[10] X.F. Peng, G.P. Peterson, Convective heat transfer and flow friction for water flow in microchannel structures, Int. J. Heat Mass Transf. 39 (12) (1996) 2599–2608.

[11] M. Choi, K. Cho, Effect of the aspect ratio of rectangular channels on the heat transfer and hydrodynamics of paraffin slurry flow, Int. J. Heat Mass Transf. 44 (1) (2001) 55–61.

[12] Y. Sui, C.J. Teo, P.S. Lee, Y.T. Chew, C. Shu, Fluid flow and heat transfer in wavy microchannels, Int. J. Heat Mass Transf. 53 (13) (2010) 2760–2772.

[13] H.A. Mohammed, P. Gunnasegaran, N.H. Shuaib, Numerical simulation of heat transfer enhancement in wavy microchannel heat sink, Int. Commun. Heat Mass Transfer 38 (2011) 63–68.

[14] J. Judy, D. Maynes, B.W. Webb, Characterization of frictional pressure drop for liquid flows through microchannels, Int. J. Heat Mass Transf. 45 (2002) 3477–3489.

[15] K.C. Toh, X.Y. Chen, J.C. Chai, Numerical computation of fluid flow and heat transfer in microchannels, Int. J. Heat Mass Transf. 45 (2002) 5133–5141.

[16] C. Aghanajafi, V. Vandadi, M.R. Shahnazari, Investigation of convection and radiation heat transfer in rhombus microchannels, IJRRAS 3 (2) (2010).

[17] M. Shams, M. Shojaeian, C. Aghanajafi, S.A.R. Dibaji, Numerical simulation of slip flow through rhombus microchannels, Int. Commun. Heat Mass Transfer 36 (2009) 1075–1081.

[18] P. Gunnasegaran, H.A. Mohammed, N.H. Shuaib, R. Saidur, The effect of geometrical parameters on heat transfer characteristics of microchannels heat sink with different shapes, Int. Commun. Heat Mass Transfer 37 (2010) 1078–1086.

[19] A. Tamayol, M. Bahrami, Laminar flow in microchannels with noncircular cross section, J. Fluids Eng. 132 (2010) 111201–111210.

[20] R. Chein, J. Chen, Numerical study of the inlet/outlet arrangement effect on microchannel heat sink performance, Int. J. Therm. Sci. 48 (2009) 1627–1638.

[21] H.C. Chiu, J.H. Jang, H.W. Yeh, M.S. Wu, The heat transfer characteristics of liquid cooling heat sink containing microchannels, Int. J. Heat Mass Transf. 54 (2011) 34–42.

[22] J. Li, G.P. Peterson, P. Cheng, Three-dimensional analysis of heat transfer in a micro-heat sink with single phase flow, Int. J. Heat Mass Transf. 47 (2004) 4215–4231.

[23] J. Li, G.P. Peterson, Geometric optimization of a micro heat sink with liquid flow, IEEE Trans. Compon. Packag. Technol. 29 (2006) 145–154.

[24] W. Qu, I. Mudawar, Analysis of three-dimensional heat transfer in micro-channel heat sinks, Int. J. Heat Mass Transf. 45 (2002) 3973–3985.

[25] A. Barba, B. Musi, M. Spiga, Performance of a polymeric heat sink with circular microchannels, Appl. Therm. Eng. 26 (2006) 787–794.

[26] N.R. Kuppusamy, H.A. Mohammed, C.W. Lim, Numerical investigation of trapezoidal grooved microchannel heat sink using nanofluids, Thermochim. Acta 573 (2013) 39–56.

[27] B.H. Salman, H.A. Mohammed, K.M. Munisamy, A.Sh. Kherbeet, Characteristics of heat transfer and fluid flow in micro-tube and micro-channel using conventional fluids and nanofluids: a review, Renew. Sust. Energ. Rev. 28 (2013) 848–880.

[28] E. Mat Tokit, H.A. Mohammed, M.Z. Yusoff, Thermal performance of optimized interrupted microchannel heat sink (IMCHS) using nanofluid, Int. Commun. Heat Mass Transfer 39 (10) (2012) 1595–1604.

[29] B.H. Salman, H.A. Mohammed, A.Sh. Kherbeet, Heat transfer enhancement of nanofluids flow in microtube with constant heat flux, Int. Commun. Heat Mass Transfer 39 (8) (2012) 1195–1204.

[30] H.A. Mohammed, P. Gunnasegaran, N.H. Shuaib, The impact of various nanofluid types on triangular microchannels heat sink cooling performance, Int. Commun. Heat Mass Transfer 38 (6) (2011) 767–773.

[31] H.A. Mohammed, P. Gunnasegaran, N.H. Shuaib, Influence of channel shape on the thermal and hydraulic performance of microchannel heat sink, Int. Commun. Heat Mass Transfer 38 (4) (2011) 474–480.

[32] H.A. Mohammed, P. Gunnasegaran, N.H. Shuaib, Heat transfer in rectangular microchannels heat sink using nanofluids, Int. Commun. Heat Mass Transfer 37 (10) (2012) 1496–1503.

[33] H.A. Mohammed, P. Gunnasegaran, N.H. Shuaib, Influence of various based nanofluids and substrate materials on heat transfer in microchannel heat sinks, Int. Commun. Heat Mass Transfer 38 (2) (2011) 194–201.

[34] S.V. Patankar, Numerical Heat Transfer and Fluid Flow, Hemisphere, New York, 1980.

[35] P. Gunnasegaran, H. Mohammed, N.H. Shuaib, Pressure drop and friction factor for different shapes of microchannels, Proceedings of ICEE 2009 3rd International Conference on Energy and Environment, 7–8 December 2009, Malacca, Malaysia, 2009.

[36] J.D. Anderson, Computational Fluid Dynamic: The Basics With Applications, McGraw-Hill, New York, 1995.
[37] H.A. Mohammed, P. Gunnasegaran, N.H. Shuaib, Heat transfer in rectangular microchannels heat sink using nanofluids, Int. Commun. Heat Mass Transfer 37 (2010) 1496–1503.
[38] K.K. Ambatipudi, M.M. Rahman, Analysis of conjugate heat transfer in microchannel heat sink, Numerical Heat Transfer Part A Appl. 37 (7) (2000).
[39] B.O. Ergu, O.N. Sara, S. Yapıcı, M.E. Arzutug, Pressure drop and point mass transfer in a rectangular microchannel, Int. Commun. Heat Mass Transfer 36 (6) (2009) 618–623.
[40] H.S. Kou, J.J. Lee, C.W. Chen, Optimum thermal performance of microchannel heat sink by adjusting channel width and height, Int. Commun. Heat Mass Transfer 35 (2008) 577–582.
[41] J. Li, G.P. Peterson, 3-Dimensional numerical optimization of silicon-based high performance parallel microchannel heat sink with liquid flow, Int. J. Heat Mass Transf. 50 (2007) 2895–2904.